

Shot noise of a multiwalled carbon nanotube field effect transistor

F. Wu¹, T. Tsuneta¹, R. Tarkiainen¹, D. Gunnarsson¹, T. H. Wang², and P. J. Hakonen¹

¹*Low Temperature Laboratory, Helsinki University of Technology, Finland*

²*Institute of Physics, Chinese Academy of Sciences, Beijing, China*

(Dated: November 2, 2018)

We have investigated shot noise in a 6-nm-diameter, semiconducting multiwalled carbon nanotube FET at 4.2 K over the frequency range 600 - 950 MHz. We find a transconductance of 3 - 3.5 μS for optimal positive and negative source-drain voltages V . For the gate referred input voltage noise, we obtain 0.2 and 0.3 $\mu\text{V}/\sqrt{\text{Hz}}$ for $V > 0$ and $V < 0$, respectively. As effective charge noise this corresponds to $2 - 3 \cdot 10^{-5} e/\sqrt{\text{Hz}}$.

Semiconducting single-walled carbon nanotubes have been shown to provide extraordinary field effect transistors (FET) [1, 2] in which the modulation of Schottky barriers is often an important factor [3, 4]. Intrinsic performance limits of these devices due to the mobility of charge carriers have been investigated recently [5, 6, 7, 8, 9, 10]. Transconductances up to $g_m = \frac{\Delta I_{ds}}{\Delta V_g} = 8700 \mu\text{S}/\mu\text{m}$, relating the change in drain-source current I_{ds} to gate voltage V_g , have been reported in SWNTs on top of a high- κ material (SrTiO₃) [11]. It has been shown experimentally that g_m increases as ϕ^2 with the tube diameter ϕ [10]. This, however, takes place at the expense of a reduced energy gap, which sets an upper limit for the diameter of room temperature devices.

Another important issue for typical FET applications is the noise power generated by the device. Here we are interested in the uncoupled noise performance, the understanding of which is a prerequisite for the proper noise minimization with a finite source impedance. In general, the low-frequency current noise $S(\omega) = \int e^{i\omega t} \langle \delta i(t) \delta i(0) \rangle$ in a mesoscopic sample can be written as

$$S = \frac{4k_B T}{R} (1 - F) + F 2eI \coth \left(\frac{eV}{2k_B T} \right) \quad (1)$$

where R is the resistance of the sample, T is temperature, F denotes the Fano-factor, and V is the DC biasing voltage. The Fano-factor depends on transmission coefficients of the transport channels of the sample, as well as on inelastic processes causing energy relaxation, which are known to lower the shot noise [12]. The best uncoupled performance corresponds to the minimization of S/g_m^2 which yields the minimum equivalent voltage noise at the input. Here we present the first experimental determination of this noise quantity in a semiconducting nanotube device.

In our 4-K measurement setup, IV characteristics and differential conductance properties are measured in a regular two terminal configuration, supplemented with a radio-frequency noise amplification circuitry. Bias-tees are used to separate dc bias and the current-dependent noise signal at radio frequencies. We use a low-noise, cooled amplifier [13] with working frequency range of 600

- 950 MHz for suppressed $1/f$ noise. The total gain of the amplifier chain amounts to 80 dB (16 dB at 4.2 K) and the noise temperature of the whole setup is roughly 10 K; for detection, we used a zero-bias Schottky diode. A switch and a high-impedance tunnel junction are used to calibrate the gain and the bandwidth, *i.e.*, we can determine the Fano-factor of our CNT samples by direct comparison with the noise measured on a tunnel junction sample having $F = 1$.

We determine the Fano-factor at drain-source voltage V_{ds} as

$$F = \frac{S(I_{ds}) - S(0)}{2eI} = \frac{1}{2eI_{ds}} \int_0^I \left(\frac{dS}{dI_{ds}} \right) dI \quad (2)$$

where $\left(\frac{dS}{dI_{ds}} \right)$ represents the differentially measured noise using a small modulation voltage of 0.5 mV at 18.5 Hz on top of V_{ds} . At large currents, this determination coincides with the ordinary definition of Fano-factor. In the intermediate bias region, there will be corrections that depend on the ratio of differential resistance $\frac{dV_{ds}}{dI_{ds}}$ to V_{ds}/I_{ds} due to thermal noise coupling, but these corrections are negligible for the analysis in this paper [14, 15]. Because the sample impedance is not matched to the preamplifier, we are able to measure shot noise only at currents of $I > I_{th}$ where $F I_{th}$ must be around 0.01 μA .

Our tube material, provided by the group of S. Iijima, was grown using plasma enhanced growth without any metal catalyst [16]. The tubes were dispersed in dichloroethane and, after 15 min of sonication, they were deposited on to thermally oxidized, strongly doped Si wafers. A tube of 4- μm in length was located with respect to alignment markers using a FE-SEM Zeiss Supra 40. Subsequently, Ti contacts of width 900 nm were made using standard overlay lithography: 10-nm titanium layer was covered by 70 nm Al in order to facilitate proximity induced superconductivity at subkelvin temperatures. The length of the tube section between the contacts was 1200 nm. The electrically conducting body of the silicon substrate was employed as a back gate, separated from the sample by 100 nm of SiO₂. The sample was bonded to a sample holder with miniature, 6-GHz bias tees using 25 μm Al bond wires with less than 10 nH of inductance.

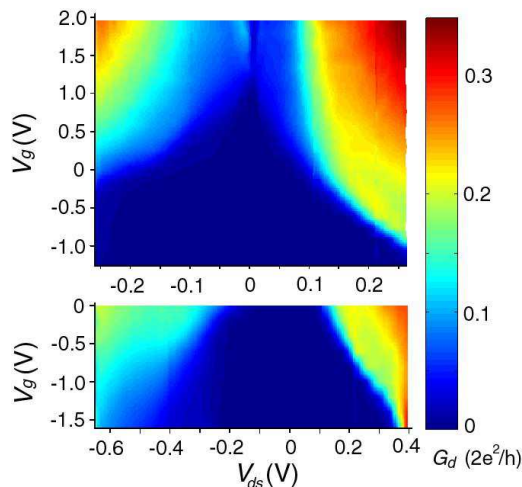


FIG. 1: (color on line) Normalized differential conductance G_d/G_0 with $G_0 = 2e^2/h$ for our semiconducting sample measured at 4.2 K on the gate V_g vs. bias voltage V_{ds} plane: the color scale is given by the bar on the right. For the sample parameters, see text.

Differential conductance $G_d = \frac{dI_{ds}}{dV_{ds}}$ for our sample is illustrated in Fig. 1 in units of $G_0 = 2e^2/h$. G_d is seen to display a roughly linear conductance, on the order of $0.1 G_0$, at voltages $V_{ds} = -0.1 \dots +0.1$ V and $V_g = 1 - 4$ V. When current is increased to $I_{ds} = 1 \mu\text{A}$, G_d becomes on the order of $0.2 G_0$, which is a typical value for metallic PECVD tubes of the same batch. Thus, there is no obvious difference in conductance between semiconducting and metallic specimens as observed in SWNT tubes [17].

Our nanotube sample is clearly n-type doped initially. Looking at $G_d(V_{ds}, V_g)$, we deduce that the charge neutrality point is located around $V_g = -1.7\text{V}$ which also corresponding to the maximum gap of 0.8 V. Using the gate capacitance $C_g = 18$ aF and total island capacitance of 0.4 fF (see below), we find that the initial shift of the Fermi-level from the charge neutrality point is approximately -0.25 V. This differs substantially from the value of $+0.4$ V that has been reported for MWNTs [18]. Typically, n-type doping in NTs has been obtained only using potassium deposition [19, 20].

The capacitance of our backgate was measured by observing Coulomb modulation in the range $V_g = 2 \dots 4$ V. The measured periodicity of 8.8 mV corresponds to 18 aF. The island capacitance $C_\Sigma = 0.4$ fF was estimated using a geometric capacitance of $C = 200$ pF/m in series with a quantum capacitance of similar magnitude along the full length $4 \mu\text{m}$. Owing to local thinning of the 100-nm SiO_2 oxide due to Al wire bonding, we used gate voltages only up to ± 4 V in our studies. In addition, we limited our measurements for currents below $5 \mu\text{A}$ which is on the same order as typical ON-state current in SWNT devices.

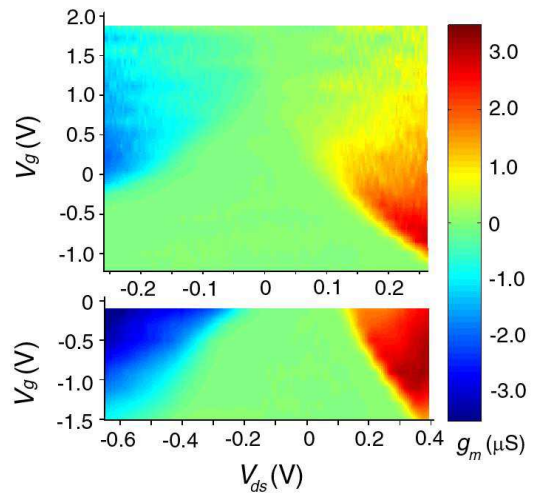


FIG. 2: Transconductance g_m as a function of bias V_{ds} and gate voltage V_g .

The model, that we employ to account for our basic findings, has been proposed and discussed in Ref. [21]. There it was conjectured that owing to band pinning at the metal-nanotube interfaces, small quantum dots are formed at the ends of the nanotube when the tube is strongly doped by the gate voltage. In our case, this is corroborated by the appearance of another (quasiperiodic) gate modulation in the range $V_g = -0.6 \dots -4$ V. This gate period changed from $\Delta V_g = 0.13$ V at $V_g \sim -1$ V to $\Delta V_g = 0.18\text{V}$ at $V_g \sim -2.5$. The size of the period is in accordance with the findings in Ref. 21, while the increase in ΔV_g in our data reflects a decrease in the dot size as V_g becomes more strongly negative.

The expected gap for a semiconducting tube of diameter $\phi = 6$ nm is approximately $V_{gap} = 0.14$ V [22]. If the extra width of the gap were due to the quantum dots at the ends of the tube, their capacitance would be about 1 aF, i.e. < 10 nm in length. Room temperature measurements indicate that the gap indeed is composed of a few smaller components, but we cannot exclude the possibility that, at some large gap value, the tube is broken into more than three quantum dots.

In CNT-FETs, the signature of charge carrier freeze-out in I_{ds} vs. V_g sweeps is the appearance of a threshold voltage, related to current by the form $I_{ds}^2 \propto V_g - V_{th}$ [11]. Using this form, we obtain $V_{th} = 0.25\text{V}$ for the pinch-off. When lowering the gate voltage towards V_{th} , the small voltage IV curves change from linear to more and more power-law-like: in the range $V_g = 1\text{V} \dots V_{th}$, the exponent varies from 1 to 3 (in Fig. 1, the exponent of G_d varies from 0 to 2, respectively).

Measured transconductance around the pinch-off region is displayed in Fig. 2 The largest magnitude of transconductance is roughly equal at positive and negative bias: $\sim 3 \mu\text{S}$ at $V > 0$ and $\sim 3.5 \mu\text{S}$ at $V < 0$. At positive bias the optimum is reached in a small region

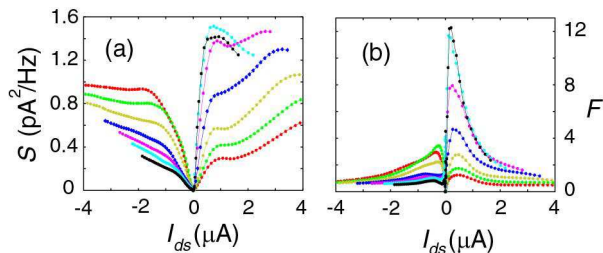


FIG. 3: Current noise S integrated over the frequency range 600 - 950 MHz. vs. current I_{ds} (a), and the corresponding Fano-factor (b). Due to lack of sensitivity, currents below $0.01 \mu\text{A}$ have been cut off from the plot. The bias voltage varies over $V_{ds} = -1.2 \dots 0 \text{ V}$ in steps of 0.2 V (from top to bottom at $V_{ds} > 0$ and from bottom to top at $V_{ds} < 0$)

of bias values around $V_{ds} = 0.37 \text{ V}$ and $V_g = -0.9 \text{ V}$ whereas at $V < 0$ the maximum value is obtained on a more extended region at $V_{ds} < -0.5 \text{ V}$ around $V_g = 0$.

Fig. 3a illustrates the measured current noise in the range $V_g = -1.2 \dots 0 \text{ V}$ which is right below the pinch-off of threshold V_{th} ; the corresponding Fano-factor is given in Fig. 3b. At large negative bias, and with large positive bias at $V_g \ll V_{th}$, the noise can be regarded as shot noise from an asymmetric double junction system [23, 24], which yields $F = (\Gamma_1^2 + \Gamma_2^2)/(\Gamma_1 + \Gamma_2)^2 < 1$ where Γ_1 and Γ_2 refer to tunneling rates in the two tunnel barriers. At small V_{ds} , especially at $V_{ds} > 0$, the measured noise is strongly peaked, and the corresponding Fano-factor reaches $F = 12$ at its maximum. This behavior may be an indication of noise due to inelastic co-tunneling as argued by Kouwenhoven and coworkers in a SWNT quantum dot at small bias [25]. In our case, however, we believe that a more likely explanation is due to a bias-dependent fluctuator that modulates the transmission at one of the contacts [26]. According to this model, the peak in the noise vs. current reflects the movement of the corner frequency of the Lorentzian fluctuation spectrum across the frequency band of the measurement. Initially, the noise increases when the corner frequency approaches the measurement band from below. The decrease at large currents is because the total integrated noise over the Lorentzian spectrum is fixed, and as the corner frequency continues to grow, the noise per unit band has to decrease [26]. Thus, we argue that there are bias-dependent fluctuators in metal-nanotube systems with tunneling rates in the GHz regime.

The overall noise characteristics of our device are illustrated in Fig. 4a. By multiplying S with $1/g_m^2$, we may convert the measured current noise into voltage noise at the gate, which is displayed in Fig. 4b. Here we assume that the electrical properties of the tube do not change with frequency up to 800 MHz, as indicated by the experiments by Burke and coworkers [27]. The lowest-noise region of operation is marked by A, which is very close to

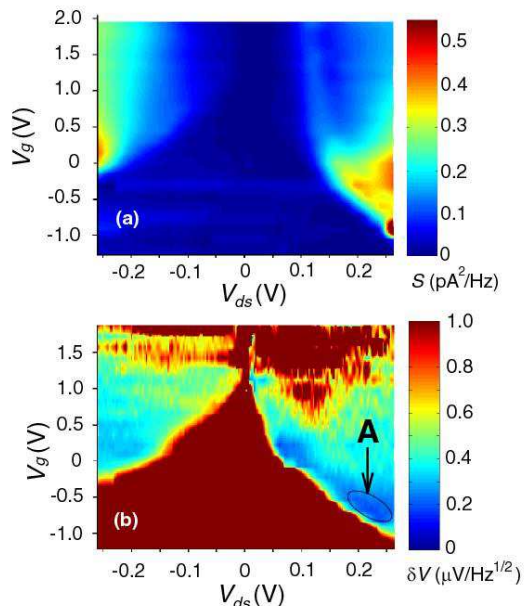


FIG. 4: a) Current noise S over V_g vs. V_{ds} plane. b) Noise power of (a) converted into input voltage noise by dividing by g_m^2 . The region of smallest noise has been denoted by an ellipsoid.

the region of maximum g_m . However, since the variation of g_m is rather slow with V_{ds} and V_g , the optimum noise is located at a local minimum of noise power. Note that, even though negative bias provides larger g_m and smaller Fano-factors, the smallest input equivalent voltage noise δV_g is found at $V > 0$, because I_{ds} is much smaller at optimum regions at $V > 0$ than at $V < 0$.

At point A, we find $\delta V_g = 0.2 \mu\text{V}/\sqrt{\text{Hz}}$. This input voltage noise, in turn, can be converted into charge noise at the gate, which yields $\delta q_g = 20 \mu\text{e}/\sqrt{\text{Hz}}$. At negative bias, our results are about 30 % worse, *i.e.* $\delta q_g = 30 \mu\text{e}/\sqrt{\text{Hz}}$. These values are close to the results obtained in RF-SET setups using impedance matching [28]. Note that no matching circuits have been employed here and that the noise has been measured over a large band of 600 - 950 MHz. In a RF-SET setup with hundreds of parallel SET's, a bandwidth of 1 GHz has been achieved, but with a limited charge sensitivity of $\delta q_g = 2 \text{ me}/\sqrt{\text{Hz}}$ due to a large input capacitance [29]. Thus, our results suggest that nanotube FETs based on MWNTs may be employed as sensitive charge detectors at high frequencies, rivaling the performance of RF-SETs.

Semiconducting nanotube devices are often described in terms of field-effect (FE) mobility $\mu_{FE} = \frac{L}{C_g^*} \frac{\partial G}{\partial V_g} = \frac{L}{C_g^* V_{ds}} \frac{\partial I}{\partial V_g}$ where C_g^* denotes gate capacitance per unit length [11]. This quantity is employed for the description of the "bulk" properties of the tube when the contribution from the contacts can be neglected. In our case, even though the length of the tube is not extremely large, the

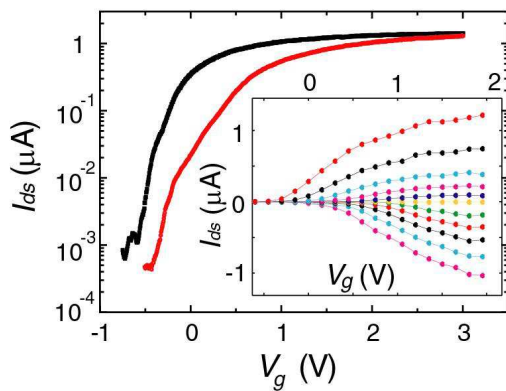


FIG. 5: Nanotube current as a function of gate V_g bias voltage $V_{ds} = +0.135$ V (\square) and $V_{ds} = -0.135$ V (\circ). The inset displays a set of current traces on linear scale measured when at V_{ds} has been stepped from -0.13 V to 0.13 V by 26 mV (from bottom to top).

resistance of the tube should dominate close to the pinch-off of the device. Gate sweeps at $V_{ds} = \pm 0.135$ V are illustrated in Fig. 5. From the figure we may read at 0.1 μ A that conductance I_{ds}/V_{ds} changes by decade/ 250 mV and by decade/ 500 mV at positive and negative bias, respectively. This fact that the threshold is sharper at $V_{ds} > 0$ is visible also from the inset of Fig. 5 which displays a set of current traces vs. V_g measured with stepping V_{ds} over -0.13 V to 0.13 V. These data at 4.2 K yield for the maximum FE-mobility $\mu_{FE} = 1$ m²/Vs which falls short by a factor of > 100 from the value extrapolated for $\phi = 6$ nm using temperature-scaled data of Ref. 10 measured above 50 K for SWNTs with $\phi = 1 - 4$ nm. This discrepancy indicates that our MWNTs are more strongly diffusive than typical semiconducting SWNTs.

In summary, we have presented first noise investigations on semiconducting nanotube FETs. We find noise behavior that varies between sub- and super-Poissonian values. The sub-Poissonian values are consistent with the double Schottky barrier configuration while the super-Poissonian results indicate the presence of two level fluctuators with bias-dependent switching rates exceeding 1 GHz. For the input referred noise, expressed in terms of charge noise on the gate, we find $2-3 \cdot 10^{-5} e/\sqrt{\text{Hz}}$. Thus, these devices may challenge regular aluminum-based RFSETs as the ultimate charge detectors.

We thank S. Iijima, A. Koshio, and M. Yudasaka for the carbon nanotube material employed in our work. We wish to acknowledge fruitful discussions with L. Lechner, M. Paalanen, B. Placais, and L. Roschier. This work was supported by the TULE programme of the Academy of Finland and by the EU contract FP6-IST-021285-2.

- [1] S.J. Tans, A. R. M. Verschueren, and C. Dekker, *Nature* **393**, 49 (1998).
- [2] A. Javey, J. Guo, Q. Wang, and M. Lundstrom, H. Dai, *Nature* **424**, 654 (2003).
- [3] S. Heinze, J. Tersoff, R. Martel, V. Derycke, J. Appenzeller, and Ph. Avouris, *Phys. Rev. Lett.* **89**, 106801 (2002).
- [4] J. Appenzeller, J. Knoch, V. Derycke, R. Martel, S. Wind, and Ph. Avouris, *Phys. Rev. Lett.* **89**, 126801 (2002).
- [5] A. Javey, J. Guo, M. Paulsson, Q. Wang, D. Mann, M. Lundstrom, and H. Dai, *Phys. Rev. Lett.* **92**, 106804 (2004).
- [6] T. Dürkop, S. A. Getty, Enrique Cobas, and M. S. Fuhrer, *Nano Lett.* **4**, 35 (2004).
- [7] H. Cazin d'Honinchtun, S. Galdin-Retailleau, J. Sée, and P. Dollfus, *Appl. Phys. Lett.* **87**, 172112 (2005).
- [8] Yung-Fu Chen and M. S. Fuhrer, *Phys. Rev. Lett.* **95**, 236803 (2005).
- [9] Z. Chen, J. Appenzeller, J. Knoch, Yu-ming Lin, and Ph. Avouris, *Nano Lett.* **5**, 1497 (2005).
- [10] X. Zhou, Ji-Yong Park, S. Huang, J. Liu, and P. L. McEuen, *Phys. Rev. Lett.* **95**, 146805 (2005).
- [11] B. M. Kim, T. Brintlinger, E. Cobas, M. S. Fuhrer, Haimei Zheng, Z. Yu, R. Droopad, J. Ramdani, and K. Eisenbeiser, *Appl. Phys. Lett.* **84**, 1946 (2004).
- [12] Ya.M. Blanter, M. Büttiker, *Phys. Rep.* **336**, 1 (2000).
- [13] L. Roschier and P. Hakonen, *Cryogenics* **44**, 783 (2004).
- [14] For details, F. Wu, *et al.*, to be published in AIP Conference Proceedings series: LT24, 10 - 17 August 2005, Orlando, Florida, USA, 2005.
- [15] At liquid helium temperature, the crossover between thermal and shot noise takes place at $V_{ds} \sim 1$ mV, which is a small voltage compared with typical V_{ds} values employed in our measurements.
- [16] A. Koshio, M. Yudasaka, and S. Iijima, *Chem. Phys. Lett.* **356**, 595 (2002).
- [17] See, *e.g.*, P. McEuen, M. Bockrath, D. Cobden, Y.-G. Yoon, and S. Louie, *Phys. Rev. Lett.* **83**, 5098 (1999).
- [18] This is with a typical oxygen doping. See M. Kruger, M. R. Buitelaar, T. Nussbaumer, C. Schonenberger, and L. Forro, *Appl. Phys. Lett.* **78**, 1291 (2001).
- [19] Marc Bockrath, J. Hone, A. Zettl, Paul L. McEuen, Andrew G. Rinzler, and Richard E. Smalley, *Phys. Rev. B.* **61**, 10606 (2000).
- [20] J. Appenzeller, J. Knoch, M. Radosavljević, and Ph. Avouris, *Phys. Rev. Lett.* **92**, 226802 (2004).
- [21] J. Park and P. McEuen, *Appl. Phys. Lett.* **79**, 1363 (2001).
- [22] See, *e.g.*, R. Saito, G. Dresselhaus, and M.S. Dresselhaus, *Phys. Rev. B* **61**, 2981 (2000).
- [23] See, *e.g.*, A.N. Korotkov, D.V. Averin, K.K. Likharev, and S.A. Vasenko, in H. Koch and H. Lübbig, eds., *Single-Electron Tunneling and Mesoscopic Devices* (Springer, Berlin, 1992), p. 45.
- [24] M. J. M. de Jong and C. W. J. Beenakker, *Physica A*, **230**, 219 (1996).
- [25] E. Onac, F. Balestro, B. Trauzettel, C. Lodewijk, and L. Kouwenhoven, *Phys. Rev. Lett.* **96**, 026803 (2006).
- [26] R. Tarkiainen, L. Roschier, M. Ahlskog, M. Paalanen, and P. Hakonen, *Physica E* **28**, 57 (2005). Note that the

corner frequency of the fluctuator may go down or up with the bias and the result is qualitatively the same.

- [27] Z. Yu and P. J. Burke, *Nano Lett.* **5**, 1403 (2005).
[28] L. Roschier, P. Hakonen, K. Bladh, P. Delsing, K.W. Lehnert, L. Spietz, and R.J. Schoelkopf, *J. Appl. Phys.*

95, 1274 (2004).

- [29] S. Gustavsson, D. Gunnarsson, and P. Delsing, *Appl. Phys. Lett.* **88**, 153505 (2006).